Cell. Mol. Life Sci. 63 (2006) 1780–1789
1420-682X/06/151780-10
DOI 10.1007/s00018-006-6129-0

Cellular and Molecular Life Sciences

Research Article

Translation control of UCP2 synthesis by the upstream open reading frame

C. Hurtaud†, C. Gelly†, F. Bouillaud and C. Lévi-Meyrueis*

BIOTRAM, CNRS UPR9078, Université René Descartes, Faculté de Médecine Necker Enfants Malades, 156 rue de Vaugirard 75730 Paris (France), Fax: +33 1 4061 5673, e-mail: levi-meyrueis@necker.fr

Received 22 March 2006; received after revision 19 May 2006; accepted 8 June 2006
Online First 17 July 2006

Abstract. Uncoupling protein 2 (UCP2) belongs to a family of transporters of the mitochondrial inner membrane. *In vivo* low expression of UCP2 contrasts with a high UCP2 mRNA level, and induction of UCP2 expression occurs without change in mRNA level, demonstrating a translational control. The UCP2 mRNA is characterized by a long 5′ untranslated region (5′UTR), in which an upstream open reading frame (uORF) codes for a 36-amino-acid sequence. The 5′UTR and uORF have an inhibitory role in the translation of UCP2. The present study demonstrates that the 3′ region of the uORF is a major determinant for this inhibitory role. In this 3′ region, a single-base substitution that kept the codon sense unchanged significantly modified UCP2 translation, whereas some important amino acid changes had no effect. We discuss our results within the framework of the existing models explaining initiation of translation downstream of a uORF.

Keywords. UCP2, mitochondria, translation, 5′ untranslated region, uORF.

The mitochondrial uncoupling proteins [UCPs] are located in the mitochondrial inner membrane where they are thought to act as regulated protonophores. The proton leak catalyzed by UCP1 in mammalian brown adipose tissue is large enough to fully uncouple mitochondrial respiration from ATP synthesis. This leads to increased energy expenditure and thermogenesis. UCP2 and UCP3 are thought to lead to a moderate uncoupling, which is believed to modulate the ATP/ADP ratio for signaling purposes [1]. However, UCP2 and UCP3 seem to have arisen evolutionarily to prevent superoxide production by mitochondria [2–8]. Increases in UCP2 expression are clearly associated with situations in which oxidative stress occurs. Furthermore, *Ucp2* gene inactivation leads to an increase in oxygen radical production by macrophages, which could have both positive and negative consequences [7, 8]. Expression of UCP2 is regulated at the level of transcription: the UCP2 mRNA is expressed at variable levels in different tissues [9, 10] and variations are recorded according to nutritional or hormonal status [11]. Post-transcriptional mechanisms also exist: in response to certain stimuli, an increase in the expression of UCP2 *in vivo* can be observed without a change in UCP2 mRNA level [10]. Experiments using inhibitors of translation confirmed that this regulation occurs at a translational level. *In vivo*, UCP2 mRNA is easily detectable in many tissues, whereas protein expression is low in mitochondria, where it is hardly detectable [10]. Therefore, translation of UCP2 seems greatly inhibited *in vivo*. Expression vectors containing wild-type or mutated UCP2 cDNA, transfected into mammalian cells in culture, allowed a preliminary identification of sequences responsible for this constitutive translational inhibition. These studies identified the long sequence upstream of the UCP2 coding frame and, more precisely, the short 111-nucleotide open reading frame (ORF1) as critical for translation inhibition [10]. More recent studies have

* Corresponding author.
† These authors contributed equally to this work.

shown that the 3′ untranslated region of UCP2 mRNA, by binding to hnRNPK protein, also likely plays a role in regulating UCP2 expression [12]. ORF1 is remarkably conserved during evolution [13]. It is located 122 nucleotides downstream from the 5′ cap, contains three AUG codons in frame, and encodes a 36-amino-acid peptide whose existence has not yet been demonstrated (Fig. 1). The term ORF1 will refer in this paper to this 111-nucleotide stretch described above, whereas the term ORF2 will be used to refer in this paper to the UCP2 coding frame that encodes the full-length UCP2 peptide.

Strict application of the known biochemical model for translation in eukaryotes would make the translation of ORF2 impossible as long as ORF1 is present. Four different mechanisms could account for UCP2 production. (i) Leaky scanning occurs when the 40S ribosomal subunit fails to initiate at the AUG codon(s) of the first ORF [14]. (ii) Ribosomal shunting refers to a situation in which ribosomes bypass uAUGs before initiating translation, because of stable RNA secondary structures. This was first shown for the RNA of the cauliflower mosaic virus [15] and recently suggested for translation regulation of the membrane protein BACE-1 [16] [but see also refs. 17, 18]. (iii) Internal ribosome entry site (IRES), in which ribosomal subunits bind to an internal sequence of the mRNA in a cap-independent manner [19]. (iv) Reinitiation takes place when the 40S ribosomal subunits remain bound to mRNA after translation of ORF1, allowing reinitiation to occur at a downstream ATG codon. While several examples of reinitiation showed no strict dependence on the amino acid sequence of ORF1 – cf. GCN4 [20] and maize Lc [21] – others point to the requirement for the exact amino acid sequence of ORF1 in maintaining the downstream translation: see mammalian AdoMetDC [22], CPA-1 of *Saccharomyces cerevisiae* [23], arg-2 of *Neurospora crassa* [24] and gpUL4 of human cytomegalovirus [25, 26]. These examples illustrate how uORFs are involved in the physiological regulation of protein expression. The production of mRNAs whose translation can be induced is appropriate for a highly effective and rapid control of genes with critical biological functions. For example, the translational control of a pool of UCP2 mRNA could allow a rapid response to oxidative stress. Mutagenesis of the UCP2 mRNA produced by an expression vector was undertaken to discriminate between the different mechanisms allowing initiation of translation at ORF2.

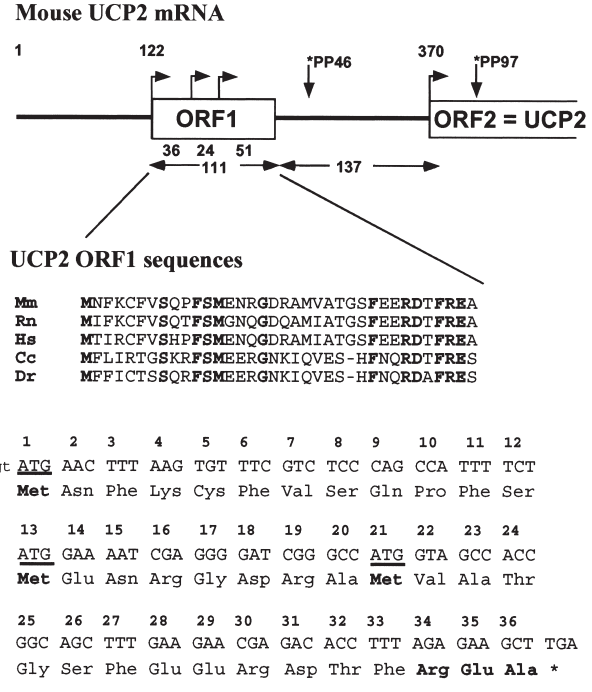

Figure 1. Upstream open reading frame (ORF1) in exon 2 of the Ucp2 gene. The scheme at the top shows the relative nucleotide position of the uORF (ORF1) and of the UCP2 coding frame (ORF2) in the UCP2 mRNA as deduced from the cDNA sequence. These relative positions are conserved in the wild-type UCP2 vector used in this study. However, due to vector sequences, the start of the actual mRNA produced in transfected cells is not coincident. The three AUG codons of ORF1 and the first AUG codon of ORF2 are indicated. *PP46 and *PP97 indicate the modified position of the stop codon of ORF1 in these two mutated UCP2 expression vectors (see text). An alignment of amino acid sequences is shown in the middle of the figure. Mm, *Mus musculus*; Rn, *Rattus norvegicus*; Hs, *Homo sapiens*; Cc, *Carpus carpio*; Dr, *Danio rerio* (zebrafish). Conserved amino acids are shown in bold. The lower part shows nucleotide and amino acid sequences of the *mUcp2* gene: the three ATGs of the nucleotide sequence are underlined. The 36 amino acids of the putative polypeptide encoded are numbered. A *Hind*III site (AAGCTT) overlaps with the last two codons; this restriction site was used to create the pUCP2-ORF1 deletion mutant [10].

Materials and methods

Media, chemicals and antibodies. Aprotinin, bestatin, leupeptin, pepstatin, phenylmethylsulfonyl fluoride (PMSF), bicinchoninic acid kit for protein determination (BCA1), and rabbit, mouse and goat horseradish-peroxidase-conjugated antibodies were from Sigma. Dulbecco's modified Eagle's medium (DMEM), Ham's F12 medium, phosphate-buffered saline (PBS), fetal calf serum (FCS), penicillin, streptomycin, geneticin (G418), and TRIzol Reagent were from Invitrogen. Cytochrome c antibodies were from Santa Cruz Biotechnology (TEBU). UCP2 antibodies used (605 or 606) have been described before [10].

Plasmid constructions and site-directed mutagenesis. The expression vector pUCP2 containing the complete mouse UCP2cDNA (1566 bp) in the pcDNA3.1 plasmid (Invitrogen) and the pUCP2-ORF1 expression vector where an important deletion removed nucleotides 1–228 from the UCP2 mRNA, including therefore the ORF1 sequence (Fig. 1), have been described previously [10]. Site-directed mutagenesis was performed using the Quick-

Change multi-site-directed mutagenesis kit (Stratagene) to introduce individual mutations in the ORF1 (Table 1). To generate PP46, the primer used to create PP97 was used in combination with a second primer inserting a nucleotide after codon 46, thus creating a new stop codon.

For the use of green fluorescent protein (GFP) as a reporter gene, the ORF1-ORF2 (1–11) and ORF1m-ORF2 (1–11) fragments (326 bp) were obtained by PCR using the sense 5′ GCCTTCTGCACTCCTGTGTT 3′ and antisense 5′ TTGGGGGCACATCTGTGGCC 3′ primers. Subsequent cloning in frame with the Cycle 3 GFP sequence in the pcDNA3.1/CT-GFP-TOPO vector (Invitrogen) created an expression vector with the 5′-untranslated region (5′UTR) of the UCP2 mRNA in front of the sequence coding for a fusion protein with amino acids 1–11 of UCP2 fused to the GFP.

The bicistronic plasmid pCREL described by Huez et al. [27] was kindly provided by Dr. A.C. Prats. In this plasmid, the two luciferase genes, *Renilla* luciferase [LucR] and firefly luciferase [LucF], are controlled by the cytomegalovirus (CMV) promoter and separated by the encephalomyocarditis virus (EMCV) IRES. For construction of pCRUL, *Nhe*I restriction sites were generated ahead of the FLuc sequence by mutation of the *Nco*I site and in pUCP2 ahead of the ATG of UCP2. By using the *Bam*HI and *Nhe*I restriction sites, the EMCV IRES was replaced by the UCP2 5′UTR sequence amplified on pUCP2 from the *Bam*HI site ahead of the 5′UTR sequence until the *Nhe*I site. When digested sites were repaired, their ligation generated the control pCRL vector containing no IRES. All the constructs were sequenced.

Cell culture. The simian kidney epithelial cell line (COS-7) and the Chinese hamster ovary (CHO-K1) cells were maintained in DMEM or Ham's F12 medium supplemented with 10% FCS, respectively, 100 IU/ml penicillin and 50 µg/ml streptomycin. The cells were grown in a humidified atmosphere of 5% CO_2. Medium was changed every 2 days and cultures were serially passaged by trypsinization every 5–7 days.

Transient transfection. Approximately 7×10^5 cells (COS-7 or CHO-K1) were seeded per 60-mm dish and allowed to grow without antibiotics to 90% confluency before their transfection with 10 µl of LipofectAMINE 2000 and 4 µg of DNA in Opti-MEM medium. According to the manufacturer's instructions, the transfection mixture was replaced with complete culture medium after 5 h. After 23 h in culture, transfected cells were harvested for UCP2 mRNA, mUCP2 protein quantitation or cell fluorescence measurement.

With the UCP2 expression vectors, each mutant was used in at least four independent transfection experiments. Transfection with the wild-type pUCP2 expression vector was included in each experiment as a reference.

Preparation of cellular extracts. Cells harvested in PBS were collected by centrifugation and resuspended in lysis buffer (50 mM Tris pH 7.8, 150 mM NaCl, 1% Nonidet P-40) in the presence of the same protease inhibitor mix as above. After 10 min incubation at 37 °C, unsolubilized material was eliminated by a 20-min centrifugation at 10,000 g.

Table 1. mUCP2 mutants in uORF.

Name	ATG 1	ATG 13	ATG 21	3′ end	Mutation
Wild type	ATG	ATG	ATG	TTT AGA GAA GCT TGA	
ATG1	ATC	- - -	- - -	- - - - - - - - - - - - - - -	initiation at 13
ATG2	- - -	AGG	- - -	- - - - - - - - - - - - - - -	Met 13/Arg
ATG3	- - -	- - -	TTG	- - - - - - - - - - - - - - -	Met 21/Leu
wo ATG	ATC	AGG	TTG	- - - - - - - - - - - - - - -	no initiation
ATG3/stop	- - -	- - -	TAG	- - - - - - - - - - - - - - -	termination at 21
R34/L	- - -	- - -	- - -	- - - CTA - - - - - - - - -	Arg 34/Leu
E35/K	- - -	- - -	- - -	- - - - - - AAG - - - - - -	Glu 35/Lys
A36/P	- - -	- - -	- - -	- - - - - - - - - CCT - - -	Ala 36/Pro
A36/A	- - -	- - -	- - -	- - - - - - - - - GCG - - -	Ala 36/Ala
A36/S1	- - -	- - -	- - -	- - - - - - - - - TCA - - -	Ala 36/Ser
A36/S2	- - -	- - -	- - -	- - - - - - - - - TCT - - -	Ala 36/Ser
ΔFREA	- - -	- - -	- - -	[ ] - - -	last 4 codons deleted
Δ21–36	- - -	- - -	[	] - - -	last 16 codons deleted
PP46	- - -	- - -	- - -	- - - - - - - - - - - - GGA	longer ORF1 : 46 codons
PP97	- - -	- - -	- - -	- - - - - - - - - - - - GGA	longer ORF1 : 46 codons

Nucleotide mutations were introduced which modified either of the three initiator methionines or one of the four codons of the C-terminal end. Deletions were created which altered the length of the amino peptide sequence.

Quantitation of protein and mRNA. Cellular proteins (30 µg) were analyzed by Western blot using the hUCP2-606 antibody and the cytochrome c antibody following a procedure described previously [10]. Signals were detected and quantified with a CCD camera in the Gene Gnome apparatus (Syngene). The protein UCP2 signal was normalized using the corresponding cytochrome c value.

Northern analysis of total RNA extracted with the TRIzol reagent from cell culture (20 µg) or transfected cells (5 µg) was carried out as described previously [10]. The UCP2 mRNA signal was quantified using a Packard instant imager, then normalized using the corresponding 18S rRNA.

Flow cytometry. After 23 h in culture, approximately 3×10^5 transfected cells were harvested in 1 ml DMEM supplemented with 5% fetal calf serum so that 1.5×10^4 cells could be analyzed per minute in an EPICS XL-MCL flow cytometer (Coulter Electronics). Green fluorescence of the cycle 3 GFP or fusion protein was excited at 488 nm and its emission was detected in the FL1 channel using a 525-nm band pass filter.

Dual luciferase assay. LucF and LucR were measured using the Promega DLR Assay System which allows simultaneous measurement of both luciferase activities. Twenty-four hours after transfection of COS-7 cells in 12-well dishes, the cells were washed with PBS and lysed by addition of 250 µl of passive lysis buffer. After protein quantification in the supernatant of a 5-min centrifugation at 10,000 g at 4 °C, protein (20 µg) was added to 100 µl of LARII and LucF activity was measured for 10 s. After addition to the same tube of 100 µl of Stop and Glo Buffer, which stops the LucF reaction and contains the LucR substrate, LucR activity was measured for 10 s. The chemiluminescence signal was measured in a Berthold luminometer.

Results

The protein-to-mRNA ratio as a measure of translation efficiency. The use of different mutated plasmids (Table 1) derived from the UCP2 expression vector (pUCP2) resulted in variable protein and mRNA levels (Fig. 2a–c). In these transient expression experiments it was possible to detect the UCP2 using cellular homogenates. Therefore, all the UCP2 produced was detected regardless of its intracellular location. Mutagenesis of the 5′UTR of the UCP2 mRNA was expected to change the protein expression level. In contrast, that the different expression vectors would produce slightly variable UCP2 mRNA levels was unexpected. The reason for this is unknown but seems to be linked to the vector sequence and not to the plasmid preparation since it was reproduced with different plasmid preparations of the same vector. Although these mRNA variations did not reach statistical significance, a simple quantification of UCP2 protein level could not accurately reflect the UCP2 mRNA translation efficiency. The protein-to-mRNA ratio (Fig. 2d) was thus used to estimate the relative translational efficiency of the various mutated forms of the UCP2 mRNA (UCP2 yield). For an easier comparison between the wild-type and mutants, a change of scale was made by multiplying all values by the constant that set the value of the UCP2 yield of the wild-type vector equal to 1 (Figs. 2–4). Probing the mRNA in Northern blots also ensured that the mRNA transcripts produced from these constructs were full-length, and eliminated the possibility that some translational effects would be ascribed to accumulation of 5′ shortened mRNAs (Fig. 2a). We checked for the relevancy of collecting cells 23 h after transfection by examining the kinetics of appearance of mRNAs with the wild-type and two mutants A36/S1 and ATG3/stop giving, respectively, the highest or the lowest level of mRNA. There were no variations in the kinetics of mRNA accumulation (data not shown), thus validating our protocol.

The woATG mutant was presented in a previous report [pUCP2-ATG in ref. 10]. The change in UCP2 yield with the woATG mutant shown here (Fig. 2d) is not quantitatively in agreement with this previous study [10]. The present evaluation is certainly closer to reality than the high values obtained previously [10] since these earlier studies used autoradiographic films whose quantitative reliability could be questioned. The same was observed with the physiological induction of UCP2 in mice [compare refs. 10 and 28]. Another mutant with a large deletion in the 5′UTR of the UCP2 mRNA leading to the loss of uORF and considerable shortening of the 5′UTR (pUCP2-ORF1) had also been used [10]. The UCP2 yield of this deletion mutant was also re-evaluated and whereas a previous study (made by autoradiography) suggested that UCP2 translation might be fifty times more efficient, the present measurement system downgraded this factor to 10.7 ± 2.9 in CHO cells ($n = 11$) and 7.5 ± 1.9 in COS cells ($n = 12$). It should be noted that both methods indicated that the shortening of the 5′ end has more effect than the mere suppression of ATGs (woATG).

Mapping critical sites within ORF1. From our previous work, we expected that decreasing the probability of translation initiation at the ORF1 would increase the UCP2 yield. This was explored further (Fig. 2d). Suppression of any single ATG codon caused no increase in the UCP2 yield (ATG1, ATG2, ATG3). Suppression of two ATGs (ATG1-2, ATG2-3) resulted in a significant stimulation, as did suppression of all ATGs (woATG).

However, the strongest stimulation (an about threefold increase in UCP2 yield) was obtained after truncation of the ORF1 by replacing the third ATG codon by a stop codon (ATG3/stop). Identical results were obtained after transfection of CHO-K1 or COS-7 cells.

Shortening the ORF1 by the ATG3/stop mutation lengthened the intercistronic region between ORF1 and ORF2 (UCP2 coding sequence) from 137 to 185 nucleotides.

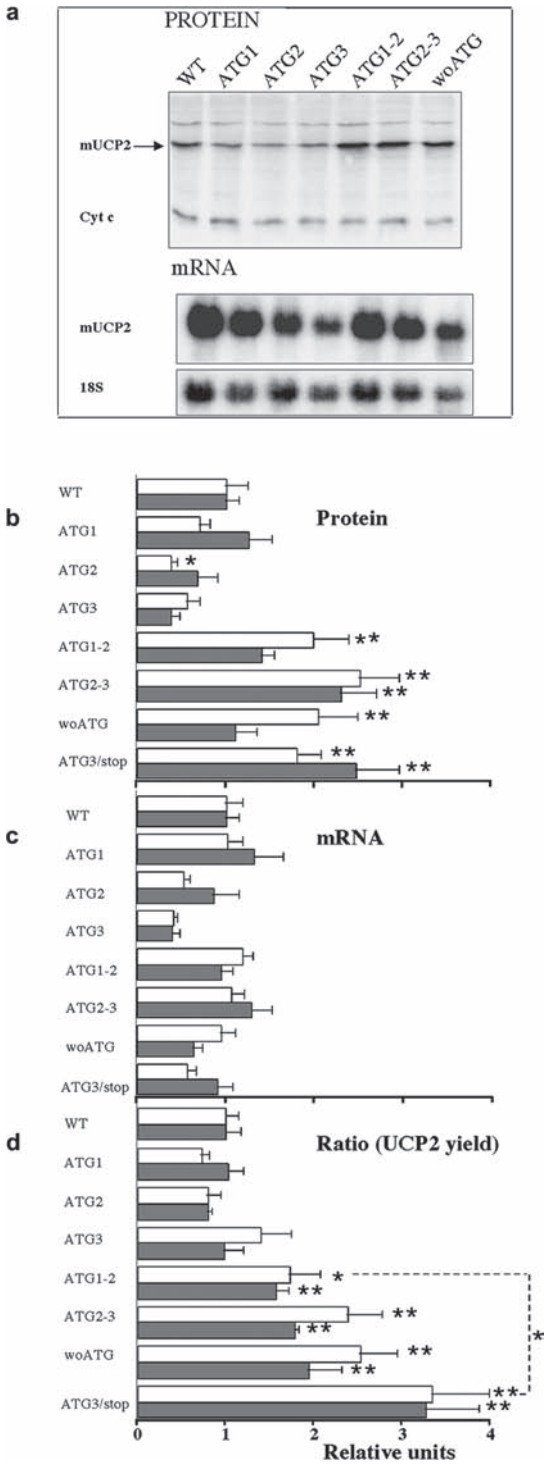

The deletion of the nucleotide sequence coding for this C-terminal part of ORF1 (48 nucleotides) in mutant Δ21–36 restored the normal space (137 nt) between the end of the truncated ORF1 and the UCP2 initiating codon. This did not restore inhibition (Fig. 3). Replacing the normal stop codon by a glycine codon displaces termination at the following stop codon. This results in a longer ORF1 now containing 46 codons (PP46) and in a shortened intercistronic sequence (107 nucleotides). This shortening did not decrease UCP2 yield (Fig. 3). These results do not support the hypothesis that the UCP2 yield depends on the length of the intercistronic sequence between ORF1 and ORF2. Another mutant was produced in which the translation of ORF1 continues to a stop codon within the UCP2 coding sequence (PP97). This mutation significantly reduced UCP2 translation but did not abolish it (Fig. 3).

Following the previous observations, the 3′ end of ORF1 was modified by several mutations. The conservation of the last amino acids involves two charged amino acids arginine 34 and glutamate 35 (Fig. 1). Conversion of the arginine 34 codon into a leucine codon (R34/L) slightly increased the UCP2 yield (Fig. 3). Inversion of the amino acid charge at codon 35 (E35/K) had a similar but not significant effect. Change of alanine 36 into proline (A36/P) or deletion of the last four codons (ΔFREA) did not change the UCP2 yield. In contrast, the synonymous mutation A36/A significantly increased UCP2 yield. Moreover, introduction in the same place of a serine, the amino acid found in fish ORF1, with the two synonymous mutants (A36/S1 or A36/S2) resulted in significantly different effects. These results suggested that the nucleotide sequence, more than the amino acid sequence, determines the ORF1 effect on UCP2 yield.

ORF1 regulates translation of a reporter gene. In the following experiments, most of the mUCP2 coding sequence was replaced by the GFP reporter gene in order to test the inhibitory effect of the ORF1 in another context. mUCP2 5′ UTR and the first 33 nucleotides of the

Figure 2. Transient transfection with UCP2 expression vectors. (*a*) An example of Western blot and Northern blot analysis after transient transfection of CHO-K1. No UCP2 mRNA could be detected in CHO-K1 or COS-7 cells. No cross-reacting band was detected at a similar molecular weight with untransfected COS-7 or CHO-K1 cells in Western blots. (*b–d*) Quantitative evaluation of the effect of the mutated versions of ORF1 on UCP2 protein (*b*), UCP2 mRNA (*c*) and protein/mRNA ratio (*d*). The values obtained after transient transfection of CHO-K1 (in white) or COS-7 (in gray) cells were determined as described in Materials and methods, and the results are expressed as the mean ± SE of at least five independent experiments. In this figure and others, the statistical analysis was done using the Mann-Whitney test (http://faculty.vassar.edu/lowry/VassarStats.html): *$p < 0.05$, **$p < 0.01$. Unless it is clearly specified by dotted lines (*d*), statistical significance refers to comparison with the value of the wild-type (WT).

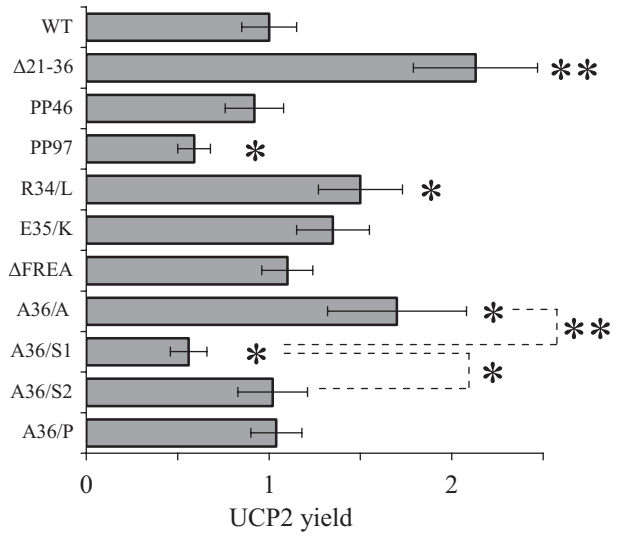

Figure 3. UCP2 yield of mutants in ORF1. The effects of the mutated versions of the ORF1 were evaluated by determination of the protein/mRNA ratio after transient transfection of CHO-K1 or COS-7 cells. The results were pooled and expressed as the mean ±SEM of 12 to 23 determinations in independent experiments; *$p < 0.05$, **$p < 0.01$. Unless clearly specified by dashed lines, statistical significance refers to comparison with the value of the wild-type (WT). The original Ala 36 codon GCG has a frequency of 0.29 in mice whereas the mutated form GCT (A36/A) has a relative frequency of 0.1. The relative frequency of TCA (A36/S1) is 0.14 and that of TCT (A36S2) is 0.19 (http://gcua.schoedl.de/compare.html) [39].

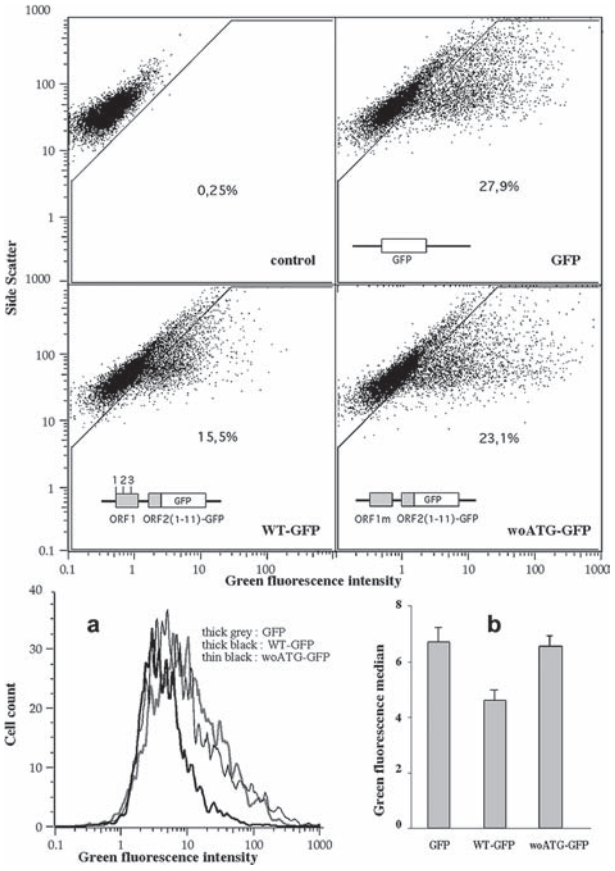

Figure 4. GFP as gene reporter of the ORF1 effect. Flow cytometry analysis of fluorescence intensity of transiently transfected COS-7 cells. Upper panel: dot plots displaying green fluorescence (FL1) intensity of the cells measured in a single experiment and represented on a logarithmic scale of 1024 channels (x-axis) versus logarithmic scale of light scatter (y-axis). FL1-positive cells considered as transfected cells are included in the polygonal area (FL1 high) defined with the control non-transfected cells. Their percentages are indicated in the windows. The GFP expression vectors used are schematized. Bottom panels: a, curves of fluorescence intensity of FL1-positive cells, discriminated by the polygonal window shown on dot plots. The curve obtained with control cells, which did not exceed 0.3%, is not shown; b, histogram interpretation, mean ± SE of the green fluorescence of positive cells (16 to 21 independent experiments).

ORF2 were cloned in frame with the GFP sequence in the pcDNA3.1/CT-GFP-TOPO expression vector, creating the WT-GFP plasmid. In this vector, suppression of the three ATGs of ORF1 gave the woATG-GFP plasmid. Green fluorescence (FL1) intensity was measured in a flow cytometer, 23 h after transient transfection of COS-7 cells. Figure 4 shows the dot plots (upper panel) and the curves (bottom panel, a) of a single representative experiment; the means of FL1 medians measured in several experiments are shown in b. The presence of the ORF1 upstream of the GFP reporter gene decreased both the percentage of FL1-positive cells (dot plots) and the mean fluorescence of FL1-positive cells (panels a and b), when compared with expression vectors in which no ORF1 was present in front of the GFP (woATG-GFP and GFP), which showed similar FL1 mean values (panel b). Thus, the inhibitory effect of the ORF1 was maintained in a new context and could be abolished by mutation of the three ATGs, as observed in mUCP2. In another series of experiments, the ATG3/stop mutation in front of the GFP was examined: the mean value of fluorescence reached 9.16 ± 0.73 (mean ± SE, $n = 5$) with this mutant whereas the WT-GFP construct gave a value of 5.40 ± 0.74 in the matched measurements. Qualitatively, this gene reporter approach remained consistent with the experiments done with the vectors derived from the full-length UCP2 mRNA. Experiments with these vectors and CHO-K1 cells gave similar results (data not shown).

The 5′UTR does not contain any IRES. The effect of the IRES of EMCV in the pCREL vector is shown by the large increase (25-fold) in the Fluc/Rluc ratio observed in comparison with the value obtained with the control (empty) vector pCRL (Fig. 5). Replacement of the EMCV sequence by the 5′UTR of mUCP2 in the intercistronic space of the pCREL bicistronic vector generated the pCRUL vector. No significant increase in relative luciferase activity was measured in COS-7 cells transiently transfected with pCRUL; an attempt made with CHO cells led to similar results. Therefore, the occurrence of an IRES in the 5′UTR is ruled out, excluding the mechanism of translation initiation of mUCP2 via an IRES.

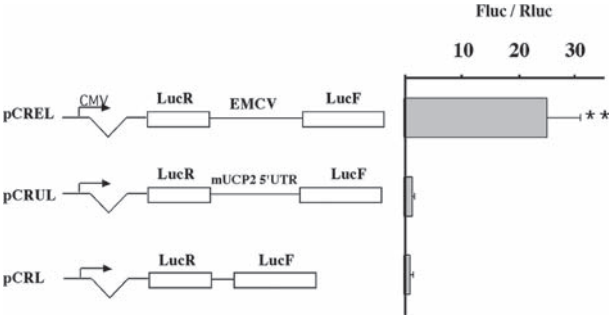

Figure 5. No evidence for an IRES. Bicistronic vector constructs contain the Renilla luciferase (LucR) gene upstream of the firefly luciferase (LucF) gene under the control of the CMV promoter. The negative control construct, pCRL, does not contain any IRES in the intercistronic space. In the pCRUL vector, the 5′UTR of mUCP2 was cloned into the intercistronic space. pCREL, the positive control for IRES function, contains the IRES of EMCV. Cells were transiently transfected and were prepared for the measurement of Rluc and Fluc activities 24 h later with the Promega DLR Assay System. Ratios of firefly luciferase activity to *Renilla* luciferase activity were determined to evaluate IRES activity. Relative IRES activities were normalized to the control vector. The results are expressed as the mean ± SE of five independent experiments, each employing triplicate transfections of COS cells, $^{**}p < 0.01$. An experiment made with CHO cells produced similar results: ratio pCRUL/pCRL = 1.4 and ratio pCREL/pCRL = 37.

Discussion

Using several models of short-term variation in UCP2 expression, previous studies have shown that the induction of UCP2 expression *in vivo* is not necessarily accompanied by a change in UCP2 mRNA [10]. Furthermore, the half-life of the protein remains constant in the several experimental models used (S. Rousset and A. M. Cassard-Doulcier, personal communication). Therefore, induction of UCP2 expression is explained by enhanced translation of a given pool of mRNA. The discrepancy between the easily detectable mRNA level and the hardly detectable protein level associated with the structure of mRNA suggested that induction of UCP2 mRNA translation in fact relies on the release of an inhibited state of translation. Before this hypothesis could be tested, two steps had to be completed: (i) the construction of mutants of the UCP2 mRNA where inhibition of UCP2 translation is lost, (ii) the validation of a protocol of induction of UCP2 translation, usable *in vitro* with transiently transfected cells. According to our hypothesis, the mutants evidenced during step 1 would show a constitutively high expression level lowering the induction factor to 1. The aim of the study presented here was to accomplish the first step.

Our previous work used the full-length UCP2cDNA inserted into the pcDNA3 expression vector. With this strategy we demonstrated the inhibitory role of the ORF1. We decided using this same transfection system to study in greater detail the inhibitory role of the ORF1 and to obtain clues about the initiation mechanisms explaining UCP2 production by the bicistronic UCP2 mRNA. The production of the entire UCP2 mRNA by the expression vector allows the conservation of all the regulatory elements putatively present in the mRNA which would be required if some long-range interaction (such as base pairing in secondary structure) is involved in the regulation of translation of UCP2 mRNA. However, it has some limitations since it restricts the analysis to cells in which endogenous UCP2 expression is minimal (null) and which may, therefore, lack other factors involved in the physiological regulation of UCP2 translation. In fact, a study with cells expressing endogenous UCP2 would have been difficult for the following reasons. (i) It would have required distinguishing the transfected from the endogenous gene product both at the mRNA and protein levels, which would have brought many complications unless a reporter gene was used. (ii) The gene reporter approach is usually considered as valid if the variations in its expression match with those of the product of the studied gene. At the time this study was initiated we were unaware of treatments able to induce endogenous UCP2 expression and validation of the gene reporter approach would have been impossible. Therefore, we had little choice about the strategy to be used, and forthcoming studies will need to address the validity of the model used here with regard to physiological induction of UCP2 expression.

UCP2 production from wild-type mRNA reveals that translation is not amenable to strict application of the scanning model which would make the first ATG codon the sole initiating codon. This may be explained by several different mechanisms: (i) the ribosomes ignore the first three ATGs of ORF1, either by leaky scanning or by a shunting mechanism bypassing the ORF1; (ii) the presence of an IRES, allowing ribosomes to enter the UCP2 mRNA downstream of ORF1, so that the ATG of UCP2 would be the first encountered; (iii) according to the reinitiation model, after ceasing translation at the stop codon of the ORF1, the ribosomal subunit (40S) remains available for a second round of initiation at the ATG of UCP2. Induction of UCP2 expression may occur through the enhancement of any of these mechanisms and the different mutations introduced in the ORF1 are expected to provide information about their relative importance.

Mechanisms explaining initiation at the ATG of UCP2. Our studies revealed that the IRES hypothesis can be ruled out (Fig. 5). Therefore, the translation of UCP2 has to be explained by ribosomes initiating scanning at the 5′ end (cap) of the UCP2 mRNA. In the PP97 mutant, the stop codon of ORF1 lies within the ORF2 sequence, a situation that makes reinitiation at the ATG codon of ORF2 impossible [14]. Therefore, leaky scanning and/or shunting must explain UCP2 production in the PP97 mutant, which has retained 60% of the UCP2 yield of the wild-type (Fig. 3). Conversely, it would be expected

that reinitiation explains about 40% of the UCP2 yield by wild-type mRNA.

General considerations about the mechanisms involved in the leaky scanning, shunting or reinitiation processes could lead to predictions about the effect of mutagenesis in the ORF1: leaky scanning or shunting rely on the probability of initiation at any of the ATGs of the ORF1. This should be heavily influenced by mutagenesis of, or around, these ATG codons. In this study, no critical ATG could be found in the ORF1 (Fig. 2), which is consistent with the similar agreement of the nucleotides surrounding each of these ATGs with the Kozak consensus sequence [29]. Accordingly, if leaky scanning explains UCP2 translation, the diminution in number of ATGs in ORF1 should increase the UCP2 yield. This is not the case when the ATG number is lowered from three to two in the single ATG mutants ATG1, ATG2 and ATG3. Moreover, with two ATGs left, ATG3/stop showed the highest UCP2 yield (Fig. 2), significantly higher than that of the ATG1-2 mutant where only one ATG (the third) is left. These results indicated that the number of ATGs present in ORF1 did not correlate negatively with the UCP2 yield. This does not favor the hypothesis of leaky scanning opposed to shunting. Reinitiation occurs after the translation of the ORF1 has taken place and this should be heavily influenced by the sequence of ORF1 itself and not uniquely by the probability of use of its ATGs. In fact, two parameters strongly influence the efficiency of the reinitiation. (i) The length of the intercistronic sequence: lengthening the intercistronic sequence increases the time available for the 40S ribosomal subunit to reacquire Met-tRNAi, described as an important point of control for reinitiation [30–32]. (ii) The length of the upstream ORF: a long uORF is an obstacle for reinitiation as reviewed in Kozak [14]. The length of the intercistronic region is not the explanation for the increase in UCP2 yield in the ATG3/stop mutant since it is also observed in the Δ21-36 mutant. Shortening ORF1 (ATG3/stop, Δ21-36, ATG1-2) increased UCP2 yield. In contrast, the results shown with the ATG2-3 (length of ORF1 unchanged) and the ATG1 (shorter ORF1) mutant do not support a hypothesis that the length of the uORF is the obstacle for the translation of the ORF2. It seems, therefore, that when parameters thought to influence either leaky scanning or reinitiation on a general basis are used, they failed to produce a consistent picture. Consequently, this calls for some specificity in the sequences of the ORF1 involved.

The 3′ domain of the uORF. It is remarkable that the ATG1-2 mutant and the ATG3/stop mutant, which result in non-overlapping sequences for ORF1, produced significantly different stimulation of UCP2 mRNA translation. In fact, these mutants pointed to the sequence downstream of the third ATG codon as a major determinant in lowering the UCP2 yield. This hypothesis was corroborated by subsequent results (Δ21-36, R34/L, A36/A, A36/S1 mutants in Fig. 3). Since cotransfection experiments did not support a possible effect *in trans* of the encoded peptide [C. Hurtaud and C. Gelly, unpublished data], the relatively high conservation of the amino acid sequence encoded by the 3′ end of ORF1 (Fig. 1) suggested an influence of the amino acid composition probably acting in *cis* through direct interaction between the peptide and translation machinery, as described in prokaryotes [33, 34] and eukaryotes [24, 35–37]. Changing the boundaries of this 3′ region (ΔFREA, PP46 in Fig. 3) had no effect, whereas the use of synonymous codons produced divergent effects (A36/A, A36/S1, A36/S2 in Fig. 3); both argue against this *cis*-acting effect of the encoded peptide. These synonymous mutants demonstrated a role for the nucleotide sequence at the 3′ end of the ORF1.

Therefore, on the one hand, translation of the region from ATG3 to the stop codon of ORF1 seems to cause inhibition of UCP2 translation since its truncation by a stop codon (ATG3/stop) or deletion (Δ21-36) of the nucleotides produced a similar increase in UCP2 yield. On the other hand, the amino acid sequence of translated ORF1 seems to be irrelevant but the nucleotide composition clearly matters. This suggests an interaction between the translation process as such and something else related to the nucleotide sequence of the mRNA. We attempted to analyze the secondary structure of the mRNA by computing [38]. Unfortunately, no clear evidence could be gathered for a link between a given structure modification and increase in the UCP2 yield (data not shown). In fact, we have no indication yet of the extent of the sequence that is relevant to examine. On the one hand, it would be legitimate to use the entire mRNA sequence, on the other, both the scanning model and the experiments with the GFP reporter gene call for a restricted analysis.

Conclusions and perspectives. It must be recalled that although the maximal increase (about threefold) obtained by mutagenesis of the ORF1 was similar to the *in vivo* increase in UCP2 expression observed upon fasting and lipopolysaccharide treatment in lung, spleen and intestine [28], we still have no guarantee that ORF1 is indeed involved in this regulation of UCP2 expression. A protocol of induction of UCP2 translation compatible with cell transfection is now required to reach a conclusion.

Our previous observations [10] and this study suggest that in considering a role of the ORF1, different mechanisms could be recruited for the stimulation of UCP2mRNA translation. They are illustrated by the two mutants, woATG and ATG3/stop. While the interpretation of the woATG mutant is obvious, the mechanism by which the ATG3/stop mutation increases the UCP2 translation remains undefined. Schematically, either the mutations in the 3′ end of the ORF1 make the initiation at the ORF1 less efficient or they stimulate reinitiation. Distinction

between these two possibilities would require further mutagenesis studies with the present system. In contrast, the use of a protocol of induction of UCP2 translation *in vitro* with the PP97 mutant would help to unravel the involvement of reinitiation. Therefore, induction of the UCP2 translation *in vitro*, its relevance to physiology, and examination of the role of the ORF1 will be the subject of our forthcoming studies.

Acknowledgements. This work was supported by the C.N.R.S. (Centre National de la Recherche Scientifique), I.N.S.E.R.M. (Institut National de la Santé et de la Recherche Médicale), the Institut de Recherches Servier, A.R.C. (Association pour la Recherche sur le Cancer) and the European Grant 'diabesity' contract number LSHM-CT-2003-503041. C. H. is supported by a PhD grant from the 'Ecole Doctorale de Physiologie et Physiopathologie' (Université Paris VI). The authors wish to thank Dr. A. C. Prats (INSERM U589 Toulouse, France) for the gift of the pCREL vector.

1 Krauss, S., Zhang, C. Y., Scorrano, L., Dalgaard, L. T., St-Pierre, J., Grey, S. T. and Lowell, B. B. (2003) Superoxide-mediated activation of uncoupling protein 2 causes pancreatic beta cell dysfunction. J. Clin. Invest. 112, 1831–1842
2 Negre-Salvayre, A., Hirtz, C., Carrera, G., Cazenave, R., Troly, M., Salvayre, R., Penicaud, L. and Casteilla, L. (1997) A role for uncoupling protein-2 as a regulator of mitochondrial hydrogen peroxide generation. FASEB J. 11, 809–815
3 Raimbault, S., Dridi, S., Denjean, F., Lachuer, J., Couplan, E., Bouillaud, F., Bordas, A., Duchamp, C., Taouis, M. and Ricquier, D. (2001) An uncoupling protein homologue putatively involved in facultative muscle thermogenesis in birds. Biochem. J. 353, 441–444
4 Vianna, C. R., Hagen, T., Zhang, C. Y., Bachman, E., Boss, O., Gereben, B., Moriscot, A. S., Lowell, B. B., Bicudo, J. E. and Bianco, A. C. (2001) Cloning and functional characterization of an uncoupling protein homolog in hummingbirds. Physiol. Genomics 5, 137–145
5 Stuart, J. A., Harper, J. A., Brindle, K. M. and Brand, M. D. (1999) Uncoupling protein 2 from carp and zebrafish, ectothermic vertebrates. Biochim. Biophys. Acta 1413, 50–54
6 Laloi, M., Klein, M., Riesmeier, J. W., Muller-Rober, B., Fleury, C., Bouillaud, F. and Ricquier, D. (1997) A plant cold-induced uncoupling protein. Nature 389, 135–136
7 Arsenijevic, D., Onuma, H., Pecqueur, C., Raimbault, S., Manning, B. S., Miroux, B., Couplan, E., Alves-Guerra, M. C., Goubern, M., Surwit, R., Bouillaud, F., Richard, D., Collins, S. and Ricquier, D. (2000) Disruption of the uncoupling protein-2 gene in mice reveals a role in immunity and reactive oxygen species production. Nat. Genet. 26, 435–439
8 Blanc, J., Alves-Guerra, M. C., Esposito, B., Rousset, S., Gourdy, P., Ricquier, D., Tedgui, A., Miroux, B. and Mallat, Z. (2003) Protective role of uncoupling protein 2 in atherosclerosis. Circulation 107, 388–390
9 Fleury, C., Neverova, M., Collins, S., Raimbault, S., Champigny, O., Levi-Meyrueis, C., Bouillaud, F., Seldin, M. F., Surwit, R. S., Ricquier, D. and Warden, C. H. (1997) Uncoupling protein-2: a novel gene linked to obesity and hyperinsulinemia. Nat. Genet. 15, 269–272
10 Pecqueur, C., Alves-Guerra, M. C., Gelly, C., Levi-Meyrueis, C., Couplan, E., Collins, S., Ricquier, D., Bouillaud, F. and Miroux, B. (2001) Uncoupling protein 2, *in vivo* distribution, induction upon oxidative stress, and evidence for translational regulation. J. Biol. Chem. 276, 8705–8712
11 Gnanalingham, M. G., Mostyn, A., Forhead, A. J., Fowden, A. L., Symonds, M. E. and Stephenson, T. (2005) Increased uncoupling protein-2 mRNA abundance and glucocorticoid action in adipose tissue in the sheep fetus during late gestation is dependent on plasma cortisol and triiodothyronine. J. Physiol. 567, 283–292
12 Ostrowski, J., Klimek-Tomczak, K., Wyrwicz, L. S., Mikula, M., Schullery, D. S. and Bomsztyk, K. (2004) Heterogeneous nuclear ribonucleoprotein K enhances insulin-induced expression of mitochondrial UCP2 protein. J. Biol. Chem. 279, 54599–54609
13 Jastroch, M., Withers, K. and Klingenspor, M. (2004) Uncoupling protein 2 and 3 in marsupials: identification, phylogeny, and gene expression in response to cold and fasting in *Antechinus flavipes*. Physiol. Genomics 17, 130–139
14 Kozak, M. (2002) Pushing the limits of the scanning mechanism for initiation of translation. Gene 299, 1–34
15 Futterer, J., Gordon, K., Sanfacon, H., Bonneville, J. M. and Hohn, T. (1990) Positive and negative control of translation by the leader sequence of cauliflower mosaic virus pregenomic 35S RNA. EMBO J. 9, 1697–1707
16 Rogers, G. W. Jr, Edelman, G. M. and Mauro, V. P. (2004) Differential utilization of upstream AUGs in the beta-secretase mRNA suggests that a shunting mechanism regulates translation. Proc. Natl. Acad. Sci. USA 101, 2794–2799
17 De Pietri Tonelli, D., Mihailovich, M., Di Cesare, A., Codazzi, F., Grohovaz, F. and Zacchetti, D. (2004) Translational regulation of BACE-1 expression in neuronal and non-neuronal cells. Nucleic Acids Res. 32, 1808–1817
18 Lammich, S., Schobel, S., Zimmer, A. K., Lichtenthaler, S. F. and Haass, C. (2004) Expression of the Alzheimer protease BACE1 is suppressed via its 5′-untranslated region. EMBO Rep. 5, 620–625
19 Vagner, S., Galy, B. and Pyronnet, S. (2001) Irresistible IRES: attracting the translation machinery to internal ribosome entry sites. EMBO Rep. 2, 893–898
20 Grant, C. M. and Hinnebusch, A. G. (1994) Effect of sequence context at stop codons on efficiency of reinitiation in GCN4 translational control. Mol. Cell. Biol. 14, 606–618
21 Wang, L. and Wessler, S. R. (2001) Role of mRNA secondary structure in translational repression of the maize transcriptional activator Lc(1,2). Plant Physiol. 125, 1380–1387
22 Hill, J. R. and Morris, D. R. (1993) Cell-specific translational regulation of S-adenosylmethionine decarboxylase mRNA: dependence on translation and coding capacity of the cis-acting upstream open reading frame. J. Biol. Chem. 268, 726–731
23 Werner, M., Feller, A., Messenguy, F. and Pierard, A. (1987) The leader peptide of yeast gene CPA1 is essential for the translational repression of its expression. Cell 49, 805–813
24 Luo, Z. and Sachs, M. S. (1996) Role of an upstream open reading frame in mediating arginine-specific translational control in *Neurospora crassa*. J. Bacteriol. 178, 2172–2177
25 Cao, J. and Geballe, A. P. (1994) Mutational analysis of the translational signal in the human cytomegalovirus gpUL4 (gp48) transcript leader by retroviral infection. Virology 205, 151–160
26 Schleiss, M. R., Degnin, C. R. and Geballe, A. P. (1991) Translational control of human cytomegalovirus gp48 expression. J. Virol. 65, 6782–6789
27 Huez, I., Creancier, L., Audigier, S., Gensac, M. C., Prats, A. C. and Prats, H. (1998) Two independent internal ribosome entry sites are involved in translation initiation of vascular endothelial growth factor mRNA. Mol. Cell. Biol. 18, 6178–6190
28 Alves-Guerra, M. C., Rousset, S., Pecqueur, C., Mallat, Z., Blanc, J., Tedgui, A., Bouillaud, F., Cassard-Doulcier, A. M., Ricquier, D. and Miroux, B. (2003) Bone marrow transplantation reveals the *in vivo* expression of the mitochondrial uncoupling protein 2 in immune and nonimmune cells during inflammation. J. Biol. Chem. 278, 42307–42312
29 Kozak, M. (1986) Point mutations define a sequence flanking the AUG initiator codon that modulates translation by eukaryotic ribosomes. Cell 44, 283–292

30 Abastado, J. P., Miller, P. F., Jackson, B. M. and Hinnebusch, A. G. (1991) Suppression of ribosomal reinitiation at upstream open reading frames in amino acid-starved cells forms the basis for GCN4 translational control. Mol. Cell. Biol. 11, 486–496
31 Kozak, M. (1987) Effects of intercistronic length on the efficiency of reinitiation by eucaryotic ribosomes. Mol. Cell. Biol. 7, 3438–3445
32 Luukkonen, B. G., Tan, W. and Schwartz, S. (1995) Efficiency of reinitiation of translation on human immunodeficiency virus type 1 mRNAs is determined by the length of the upstream open reading frame and by intercistronic distance. J. Virol. 69, 4086–4094
33 Lovett, P. S. and Rogers, E. J. (1996) Ribosome regulation by the nascent peptide. Microbiol. Rev. 60, 366–385
34 Konan, K. V. and Yanofsky, C. (1999) Role of ribosome release in regulation of tna operon expression in *Escherichia coli*. J. Bacteriol. 181, 1530–1536
35 Cao, J. and Geballe, A. P. (1996) Coding sequence-dependent ribosomal arrest at termination of translation. Mol. Cell. Biol. 16, 603–608
36 Wang, Z., Fang, P. and Sachs, M. S. (1998) The evolutionarily conserved eukaryotic arginine attenuator peptide regulates the movement of ribosomes that have translated it. Mol. Cell. Biol. 18, 7528–7536
37 Raney, A., Law, G. L., Mize, G. J. and Morris, D. R. (2002) Regulated translation termination at the upstream open reading frame in s-adenosylmethionine decarboxylase mRNA. J. Biol. Chem. 277, 5988–5994
38 Zuker, M. (2003) Mfold web server for nucleic acid folding and hybridization prediction. Nucleic Acids Res. 31, 3406–3415
39 Fuhrmann, M., Hausherr, A., Ferbitz, L., Schodl, T., Heitzer, M. and Hegemann, P. (2004) Monitoring dynamic expression of nuclear genes in *Chlamydomonas reinhardtii* by using a synthetic luciferase reporter gene. Plant Mol. Biol. 55, 869–881